EUROPEAN COMMISSION

HORIZON EUROPE PROGRAMME – TOPIC: HORIZON-CL5-2022-D2-01

FASTEST

Fast-track hybrid testing platform for the development of battery systems

Deliverable D3.1: Multiscale high fidelity modelling paradigm for physical testing virtualization

Alvaro Sanchez

Organization: ABEE

Date: [23/11/2023]

Doc.Version: [V1.0]

Funded by the European Union

Funded by the European Union under grant agreement N° 101103755. Views and opinions expressed are however those of the author(s) only and do not necessarily reflect those of the European Union or the European Climate, Infrastructure and Environment Executive Agency (CINEA) Neither the European Union nor CINEA can be held responsible for them.

Document Control Information	
Settings	Value
Work package:	WP3
Deliverable:	Multiscale high-fidelity modelling paradigm for physical testing virtualization
Deliverable Type:	Report
Dissemination Level:	Public
Due Date:	30.11.2023 (Month 6)
Actual Submission Date:	27.11.2023
Pages:	< 47 >
Doc. Version:	V1.0
GA Number:	101103755
Project Coordinator:	Alvaro Sanchez | ABEE (alvaro.anquela@abeegroup.com)

Formal Reviewers		
Name	Organization	Date
Julen Manterola	IKERLAN	07.11.2023
Iker Lopetegi	MGEP	05.11.2023

Document History			
Version	Date	Description	Author
1.0	23.11.2023	Final version 1	Alvaro Sanchez (ABEE)
1.0	27.10.2023	Sections 4.2, 4.5, part of 4.3	Laura Oca (MGEP)
1.0	06.11.2023	Cell and module level analysis by MGEP	Joanes Berasategi and Laura Oca (MGEP)
1.0	30.10.2023	Degradation modelling and validation	Igor Mele and Tomaž Katrašnik (UL)
1.0	30.10.2023	Section 5.3 and parts of sections 5.1 and 6.	Julen Manterola (IKERLAN)
1.0	07.11.2023	Section 1,2,3 and Section 4.1	Alvaro Sanchez (ABEE)

Project Abstract

Current methods to evaluate Li-ion batteries safety, performance, reliability and lifetime represent a remarkable resource consumption for the overall battery R&D process. The time or number of tests required, the expensive equipment and a generalised trial-error approach are determining factors, together with a lack of understanding of the complex multiscale and multi-physics phenomena in the battery system. Besides, testing facilities are operated locally, meaning that data management is handled directly in the facility, and that experimentation is done on one test bench.

The FASTEST project aims to develop and validate a fast-track testing platform able to deliver a strategy based on Design of Experiments (DoE) and robust testing results, combining multi-scale and multi-physics virtual and physical testing. This will enable an accelerated battery system R&D and more reliable, safer, and long-lasting battery system designs. The project's prototype of a fast-track hybrid testing platform aims for a new holistic and interconnected approach. From a global test facility perspective, additional services like smart DoE algorithms, virtualised benches, and DT data are incorporated into the daily facility operation to reach a new level of efficiency.

During the project, FASTEST consortium aims to develop up to TRL 6 the platform and its components: the optimal DoE strategies according to three different use cases (automotive, stationary, and off-road); two different cell chemistries, 3b and 4 solid-state (oxide polymer electrolyte); the development of a complete set of physic-based and data-driven models able to substitute physical characterisation experiments; and the overarching Digital Twin architecture managing the information flows, and the TRL6 proven and integrated prototype of the hybrid testing platform.

LIST OF ABBREVIATIONS, ACRONYMS AND DEFINITIONS

Acronym	Name
ASD	Acceleration spectral density
BMS	Battery Management System
BTMS	Battery Thermal Management System
BOL	Beginning of Life
CFD	Computational Fluid Dynamics
DoD	Depth of Discharge
EC	Ethylene Carbonate
EIS	Electrochemical Impedance Spectroscopy
EOL	End of Life
FEA	Finite Element Analysis
FIB	Focused Ion Beam
FRF	Frequency response
HPPC	Hybrid Pulse Power Characterisation
LFP	Lithium iron phosphate $LiFePO_4$
MOR	Model Order Reduction
MSMD	Multi-Scale, Multi-Domain
P2D	Pseudo-two Dimensional model
PBM	Physics-Based Models
PSD	Power Spectral Density
SEI	Solid Electrolyte Interphase

SEM	Scanning Electron Microscope
SOC	State of Charge
SOH	State of Health
SPM	Single Particle Model
SPMe	Extended Single Particle Model
TEM	Transmission Electron Microscope

LIST OF TABLES

LIST OF FIGURES

Table of Contents

1. EXECUTIVE SUMMARY

Deliverable D3.1 is an essential document within the FASTEST project, meticulously investigating diverse modeling approaches to ascertain the most effective methods for the project's goals in battery system development. The deliverable rigorously assesses various modeling techniques, scrutinizing their capabilities to accurately predict and enhance battery performance at multiple scales.

The document serves as a cornerstone for the project, judiciously determining which modeling techniques are most conducive to advancing the FASTEST project's objectives. By systematically comparing different methodologies, the deliverable identifies a curated set of models that promise to bring precision and efficiency to the project's research endeavors.

In shaping Deliverable D3.1, the FASTEST team has been deliberate in selecting models based on their practicality, relevance, and potential impact. This foundational work is expected to guide the project's path forward, influencing the design and execution of subsequent experiments and simulations. The deliverable is thus not only a reflection of comprehensive analytical work but also a strategic guide for the project's future modeling and testing efforts.

In conclusion, Deliverable D3.1 encapsulates a thorough selection process, highlighting the deliverable's pivotal role in steering the FASTEST project toward the adoption of robust and effective modeling techniques. These methodologies are set to underpin the project's innovative approach to battery technology, enhancing the project's contribution to the advancement of energy storage solutions.

2. OBJECTIVES

Within the FASTEST project, Deliverable 3.1 focuses on establishing advanced modeling paradigms for the virtualization of physical testing in lithium-ion batteries. The primary aim is to define and develop cell-level modeling methodologies, encompassing empirical, physics-based, and data-driven models. Emphasis is placed on comparing and analyzing these approaches to highlight their respective advantages and limitations. This analysis forms a robust foundation for understanding and selecting the most appropriate modeling approach for FASTEST PROJECT.

Delving deeper into physics-based modeling techniques, the significance of advanced models such as P2D, SPMe, and SPM is accentuated. These models are enhanced by incorporating ageing mechanisms and thermal aspects, representing a qualitative leap in the ability to predict and understand battery behavior under various operational conditions. Validating these models through correlation with experimental data is crucial to verify their accuracy, reliability, and practical applicability in predicting performance, thermal behavior, and ageing characteristics of batteries. Moreover, the project extends its scope to module-level modeling, integrating diverse and advanced modeling approaches, including mechanical aspects, and presenting electro-thermal and mechanical models that push beyond the current state-of-the-art.

This deliverable concludes with an assessment of key achievements and learnings, laying the groundwork for future research and applications of the models in the battery industry.

3. INTRODUCTION

In the realm of contemporary battery technology, the evolution towards more efficient, safe, and long-lasting energy storage systems is paramount. FASTEST project embarks on an ambitious journey to revolutionize landscape batteries through advanced modeling and virtualization techniques. Deliverable 3.1, a pivotal component of this initiative, aims to redefine the approach to battery testing and evaluation.

This deliverable focuses on the development and validation of a multiscale, high-fidelity modeling paradigm, designed specifically for virtualizing the physical testing of batteries. The objective is to construct and validate models that accurately simulate the electrochemical, thermal, and mechanical behavior of lithium-ion batteries at both the cell and module levels. Embracing a range of modeling methodologies, including empirical, physics-based, and data-driven approaches, this initiative seeks to offer a comprehensive toolkit for predicting battery performance under diverse operational conditions.

A key aspect of Deliverable 3.1 is the enhancement of traditional modeling techniques. This includes advancing physics-based models such as P2D, SPMe, and SPM, and integrating ageing mechanisms and thermal effects. Such advancements aim to create a more detailed and accurate representation of battery behavior, particularly under stress or during extended usage.

Additionally, the deliverable emphasizes the importance of rigorous model validation against experimental data. This process is critical to ensuring the reliability and practical applicability of the models for both existing and emerging battery technologies. The validation encompasses various aspects, including performance, thermal response, reliability and aging characteristics, thereby affirming the models' predictive accuracy and utility.

Deliverable 3.1 represents a collaborative effort within the FASTEST project, leveraging the diverse expertise of its partners. This collaboration is not just about resource pooling but also about embracing a multidisciplinary approach to address the complexities of battery modeling. The outcomes of this deliverable are expected to significantly contribute to the overarching goals of the FASTEST project, setting new benchmarks in battery testing and development, and advancing the field towards more sustainable and efficient energy solutions.

4. CELL LEVEL MODELLING

This section is dedicated to the exploration and evaluation of various modelling approaches that are employed to understand and predict the behavior of battery cells. In the realm of battery system development, accurate cell level modelling is indispensable for optimizing performance, safety and longevity.

Each approach offers a unique lens through which the intricate working of battery cells can be examined and characterized. Empirical models rely on observed behavior to formulate predictions, physics-based models use the foundational laws of electrochemistry and thermodynamics to capture the internal processes, and data-driven models apply sophisticated algorithms to harness the power of big data for predictive analytics.

The discussion in this section is not just theoretical but is underpinned by practical examples and case studies that demonstrate the application and efficacy of each modelling type. Through this comprehensive analysis, the aims to establish a versatile and robust modelling framework.

4.1 Types of modeling

In the dynamic field of battery technology, understanding and predicting battery behavior is crucial for innovation, efficiency, and safety. The modeling of batteries, a cornerstone of modern energy storage systems, involves a variety of approaches, each with its unique methodology and focus. These modeling techniques play a pivotal role in battery management systems, design optimization, and the advancement of battery technology.

Modeling approaches can be broadly categorized into different types such as empirical models, physics-based models, and data-driven models. Each of these approaches offers distinct insights and tools for addressing the complex nature of battery operation. While empirical models provide quick and practical solutions for real-time applications, physics-based models offer a deeper understanding of the internal electrochemical processes. On the other hand, data-driven models, leveraging the power of machine learning and big data, bring a new dimension to battery modeling, capable of handling vast and complex datasets to predict battery behaviour.

Understanding the strengths, limitations, and best use cases for each of these modelling types is crucial for researchers, engineers, and technologists working in the field of battery technology. The following sections delve into the specifics of each modelling type, providing a comparative overview that highlights their characteristics, principles, and how they integrate and complement each other in practical applications.

4.1.1 Empirical Models

Characteristics and Principles:

- Empirical models are based on correlating experimental data with output results, using mathematical and statistical formulas.
- They focus on the direct relationship between observed inputs and outputs, rather than on the underlying mechanisms governing battery behavior. [1]

Integration and Complementarity:

- In practice, they are used in applications where speed and simplicity are essential, such as in real-time control algorithms and battery management systems.
- Often, they are combined with more complex models to provide a quick initial approximation or to validate results in specific operational situations.

Application:
The Thevenin model is a widely recognized empirical model in the realm of electric vehicle battery management systems. It stands out for its simplicity and effectiveness in real-time applications. By representing the battery as an equivalent circuit comprising resistors and a voltage source, this model enables the efficient estimation of critical parameters such as the State of Charge (SoC) and State of Health (SoH). This approach is not only fundamental in providing real-time data to drivers but also plays a key role in the overall management and longevity of the battery system. [2]

4.1.2 Physics-Based Models

Characteristics and Principles:

- These models are grounded in physical and chemical laws, such as mass and energy conservation equations and electrochemical dynamics.
- They provide a detailed and accurate description of internal processes, from ionic dynamics to electrochemical reactions. [3]

Integration and Complementarity:

- Essential in research and development, where a deep understanding of the internal workings of the battery is required for innovation and optimization.
- Often used in combination with empirical and data-driven models to calibrate parameters and validate predictions under real operational conditions.

Application:
The Pseudo-Two Dimensional (P2D) model, commonly referred to as the Newman model, is a cornerstone in the field of battery materials research and development. This model provides a comprehensive view of the electrochemical processes within a battery cell, including ion transport and reaction kinetics. By allowing for detailed simulations and predictions of how changes in materials and design affect battery performance, the P2D model is instrumental in guiding the development of more efficient and durable battery cells. Companies utilize variations of this model to optimize the energy density, power capacity, and lifespan of batteries used in a wide range of applications, from consumer electronics to electric vehicles.

4.1.3 Data-Driven Models

Characteristics and Principles:

- These models apply machine learning algorithms and statistical analysis to discern patterns and predict behaviours from large volumes of data.
- Their focus is on adaptability and prediction, rather than on a detailed understanding of the underlying processes. [4]

Integration and Complementarity:

- Particularly useful in environments where a massive amount of operational data is available and significant information for prediction and analysis is sought.
- Can be used in conjunction with physical models to provide adaptive forecasts and explore new horizons in battery performance and degradation under various conditions.

Application:
In the management of large-scale energy storage systems, such as those used in grid storage or large industrial applications, data-driven models are increasingly playing a vital role. These models, often based on sophisticated machine learning algorithms, analyze vast datasets encompassing usage patterns, environmental conditions, and operational parameters. For instance, Tesla's Powerpack system employs such models to optimize the performance and longevity of its storage units. By predicting battery degradation and dynamically adjusting operational strategies, these models not only enhance the efficiency and reliability of the storage system but also reduce maintenance costs and extend the operational lifespan of the batteries. [4]. A comparison of the models with their respective advantages and disadvantages is shown in Table 1 below.

Type of Mode	Description and Applications	Advantages	Disadvantages
Empirical Models	Based on statistical correlations from experimental data. Used in real-time control and battery management systems.	- Simplicity and speed - Low computational cost - Effective for specific applications	- Limited to available data - Do not explain internal processes - Poor extrapolation capability
Physics-Based Models	Grounded in physical and chemical principles. Essential in R&D, design, and optimization of batteries.	- High level of detail and accuracy - Useful for innovation and optimization - Robust predictive capacity	- Complex and computationally expensive - Require accurate data for calibration - Less practical in real-time applications
Data-Driven Models	Use machine learning to identify patterns in large data sets. Applied in predictive analysis and advanced monitoring.	- Flexible and adaptable - Handle complex systems - Useful for large data sets	- Dependent on data quality - "Black box" with little physical interpretation - Risk of overfitting

Table 1. Model comparison

4.2 Physics-based modeling

This model is based on the mathematical framework developed by Newman *et al*. [5, 6, 7, 8]. The model can simulate any insertion cell if physical properties and system parameters are given, and is based on the porous electrode and concentrated solution theory. It is not possible to describe perfectly the complex multiphysic behaviour of batteries, and for this reason a clarification of the continuum model approach and model assumptions must be well defined to establish the model framework. More detailed information on the P2D model description can be found in [9]. This continuum model consists of a 1-D macroscopic model coupled with a pseudo dimension that is represented Figure 1. Schematic representation of the electrochemical model on a full-cell configuration

The macroscopic description of this model is defined by volume averaging over small finite volume units of microscopic quantities. As a result, the electrodes are considered as the superposition of two continua, representing the solid and the liquid phases. Moreover, the electrodes are considered as porous matrices of electrochemically reactive and electrically conductive solids. The model assumes that the electrolytic solution completely fills the voids of the porous solid matrix. This means that solid and liquid matrices are considered separately. The microscopic level describes the active material particles and is represented in the pseudo-dimension (see in Figure 1), and each electrode has one domain and two boundaries in which R = 0 corresponds to the particle core and R = 1 to the particle surface. Microscale geometries are described assuming volume-averaging theorems.

The P2D model consists of a group of nonlinear partial differential equations and algebraic equations (PDAEs) that are derived from the concentrated solution theory, the porous electrode theory, and a coupled kinetic equation for lithium-ion and electron exchange. The P2D model solves spatial and time evolution of five variables: (1) Potential ($\boldsymbol{\phi_s}$(x, t)) of lithium in the solid particles; (2) Concentration ($\boldsymbol{c_s}$(x, r, t)) of lithium in the solid particles, specifically on the surface of the solid ($\boldsymbol{c_{s,e}}$ (x, t)); (3) Potential ($\boldsymbol{\phi_e}$(x, t)) of lithium in the electrolyte; (4) Concentration ($\boldsymbol{c_e}$(x, t)) of lithium in the electrolyte and (5) Flux of lithium out of a particle ($\boldsymbol{j}$(x, t)).

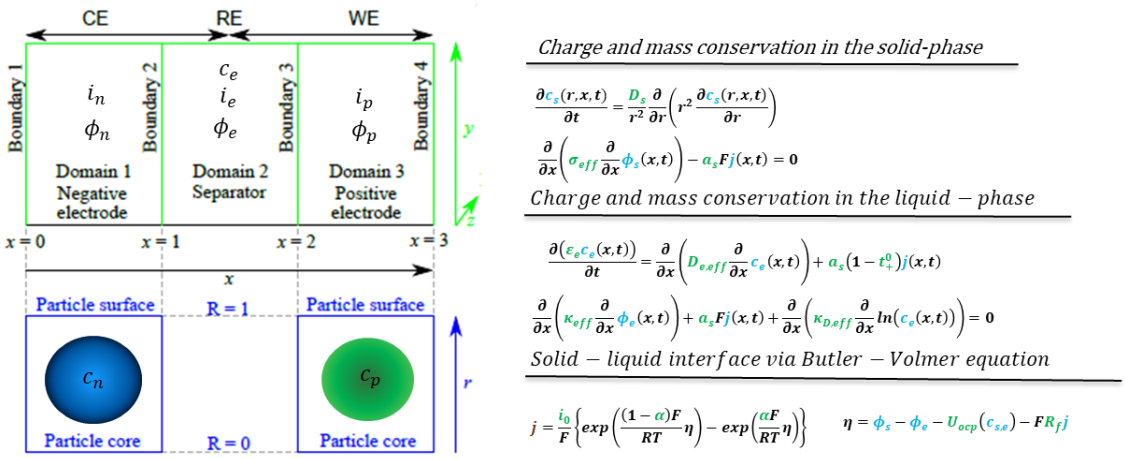

Figure 1. Schematic representation of the electrochemical model on a full-cell configuration

Blue represents the pseudo-dimension (r) in which a particle is presented. Black represents the 1D dimension (x) of the model, thicknesses of the components of the cell (3 domains and 4 boundaries). Green represents y and z dimensions that are used to calculate the cross-sectional area. CE: counter electrode; RE: reference electrode; WE: working electrode. The main equations with parameters (green) and variables (blue) highlighted in colours are shown.

In the governing equations, several assumptions are needed to describe the porous media of the electrodes and separator, commonly, the particles are assumed to be spherical, with uniform size and homogeneously distributed through the electrode. The porous media is accounted correcting the parameters with the Bruggeman exponent considering a non-ideal path through the electrode. Several authors have proposed modifications to the P2D model equations enhancing the model predictions. Some of the most relevant contributions deals with the introduction of particle size distributions [10, 11, 12], concentration dependent parameters [13], or by accounting properties of blended materials [14, 15, 16]. The inclusion of particle size distribution (PSD) [11, 12, 13] can improve the accuracy of model predictions, especially at higher C-rates and for heterogeneous electrodes. Blended materials on positive or negative electrodes have been included in next-generation LIBs to achieve higher energy densities [14, 15, 16, 17]. Carelli et al. [17] developed a model that considers a positive active material blend between LCO and NCA for a commercially available cell. They [17] claim that there is a big gap into exhaustive parametrisation of blend materials to decouple both material contributions.

In the FASTEST project, one of the main concerns to use physics-based models (PBMs) into testing virtualization (or in other cases in real-time and control-oriented applications), is the high computational cost and complexity of these models [18]. To reduce the computational cost, different simplifications have been proposed in the literature [19, 20, 21, 22, 23, 24].

The most widely used simplification of the P2D model is the Single Particle Model (SPM) [19]. The most relevant differences with the P2D are: (1) The electrolyte dynamics are neglected (this means that the solid-phase diffusion is assumed to be the slowest process and its dynamics are dominant); (2) The positive and negative electrodes are represented by a single average spherical particle; and (3) the lithium flux has a linear dependency with the input current. This model presents lower accuracy than the P2D model, especially at mid-high rates, since the electrolyte dynamics become more relevant [19, 20]. To overcome the SPM drawbacks, some authors extended the SPM to include the electrolyte dynamics [20, 21]. These models are called extended single particle models (ESPMs) or single particle models with electrolyte dynamics (SPMe-s). A canonical SPMe was derived by Marquis et al. in [20], using asymptotic reduction techniques, which was proven to be more accurate than the previously developed SPMe-s, which used ad-hoc assumptions to add correction terms to the SPM to consider the electrolyte dynamics. Marquis et. al [20] compared the P2D, SPM and SPMe models. The computational cost of the SPMe and SPM was shown to be significantly lower compared to the P2D model, and the SPMe improved the accuracy of the SPM considerably, especially at mid-high C-rates (studied up to 3C). Moreover, unlike the SPM, the SPMe maintains all the variables solved by the P2D model, at a similar computational cost of the SPM.

In addition to simplifying the P2D model to get the SPM or SPMe models explained above, model order-reduction (MOR) techniques could be employed in all these models to reduce its computational cost. Those techniques are out of the scope of

this deliverable as they will be part of the next FASTEST project tasks. However, in this section, a brief clarification of the differences between simplification and order reduction have been included. MOR techniques are methods that reduce the computational complexity of the models without adding any assumption to the original model. The main goal of MOR techniques is to obtain a ROM that keeps the same information of the (full-order-model) FOM but with lower computational burden. The PDAEs are approximated into lower order systems of ODEs and algebraic equations. Therefore, the computational efforts to obtain the time and space dependent solution can be drastically decreased. The main advantage is that they retain all the information of the internal states.

4.3 Extension to account for thermal aspects

Additionally, the P2D model can extend its validity range and predictive ability including thermal and ageing models. For thermal modelling, the most widely approach consists of adding two more variables in the original model, the heat and temperature. A macroscopic equation relates the heat generated at the microscale with the temperature variation across the cell [25, 26, 27]. Pals and Newman [28, 29] presented a one-dimensional thermal-Electrochemical model that added the energy balance equation in the form given by Bernardi et al. [30]. If the temperature is considered uniform within the cell, which is valid in small format cells [31], the macroscopic equation relates the heat generated and the temperature variation by averaged and macroscopic properties in the following form:

$$\rho C_p \frac{dT}{dt} = -\frac{hA_{cell}(T - T_{amb})}{V_{cell}} + q_{gen}$$

This equation includes three parameters related to thermal characteristics: density, ρ, heat capacity, Cp, and the convective heat transfer coefficient, h. Moreover, the temperature dependence of the electrochemical parameters is introduced by Arrhenius' law [32]. The heat generation rate, $qgen$, has four main contributions related to the microscopic scale: (1) the heat generated for kinetic reactions, (2) the reversible heat generation due to entropy changes in the electrode active material during lithium intercalation/de-intercalation, (3) the electronic and ionic ohmic heat generation due to the transport of lithium ions, and (4) the Joule ohmic heat due to the contact resistance at the boundaries [33].

The electrochemical model coupled to the macroscopic thermal equation works well for small format cells where the temperature gradient along the cell is relatively small, or when the cell is not under heavy directional cooling rates [34]. For large format cells or for battery packs, other modelling approaches can be examined which are discussed within the module level modelling.

4.4 Degradation phenomena and modelling approaches

This section will present modelling approaches to the modelling of the degradation phenomena inside the electrochemical cells and can be applied to the project's specified cell chemistry and cell generation. Since the current deliverable is due in the early stages of the project and the experimental results on the degraded cells will be available in the later stages of the project (with some of them being also under IP protection), the presented approaches will serve as a theoretical guideline for selection and later development of the relevant aging mechanisms and corresponding models.

4.4.1 Introduction

Li-ion batteries are an example of electrochemical devices with complex intra-cell transport, electrochemical, thermal and degradation phenomena. With time and increasing number of cycles, the performance and the capacity of the battery decreases. There are several factors that have an impact on the battery degradation and can be a consequence of chemical mechanisms (e.g., side reactions) and physical mechanisms (e.g., thermal stress and mechanical stress) [35]. Figure 2 schematically presents the main degradation phenomena in Li-ion batteries which can be attributed to every major component of the electrochemical cell, i.e., active material, electrolyte, additives and current collectors.

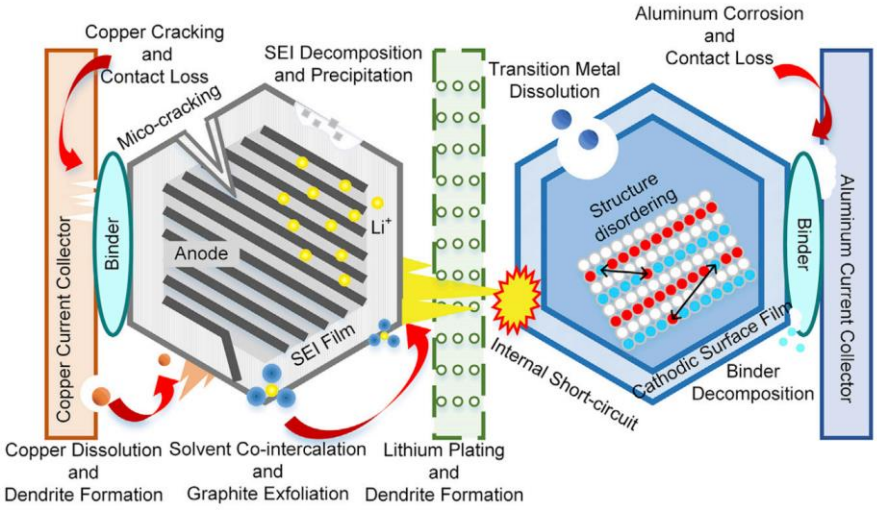

Figure 2. Schematic representation of the main degradation phenomena in Li-ion batteries. Source: [35].

The basis for accurate modelling of the degradation is an electrochemical performance PxD model with high fidelity in terms of modelling transport, electric and thermal phenomena [36] since they are strongly coupled with the degradation models.

4.4.2 LFP transport properties and aging

On the case of the cathode material $LiFePO_4$ (LFP) which is inherently phase separating material, we demonstrated significant deviations in transport properties for such materials and morphologies of secondary particles [37]. At low

charge/discharge currents particle-by-particle (de)lithiation occurs [38] where only a fraction of the electrode material is being active and therefore experiences significantly higher current densities compared to the electrode materials without the phase separation. Additionally, due to the inter-particle phase separated states, a partial cycling can occur during a single charge or discharge to the part of the active material. In [36] we further demonstrated that such effects generate additional contributions to the overall heat generation from the level of the electrochemical cell which decisively influence the entire chain of mechanisms that can lead to the outbreak of the thermal runaway of the battery.

LFP features a relatively stable crystal structure. Therefore, the capacity loss is mainly ascribed to the consumption of Li on the anode side [39, 40] (surface of the graphite and Silicon) for SEI growth and regeneration induced by graphite's inner structural deterioration or volume expansion of Silicon particles. However, Sun et al. [40] also demonstrated with XRD measurements that high discharge rates have indeed a negative effect on the structure of LFP cathode material.

4.4.3 Growth of the SEI layer

Solid Electrolyte Interphase (SEI) layer is formed during the formation cycles of the fresh battery on the surface of the anode active material (anode side in the Figure 2). Due to the low operating potential of the anode (around 0.2 V), reaction products of Li+, Li salt (e.g., $LiPF_6$) and carbonate solvent (e.g., ethylene carbonate, EC) form SEI layer [41] which protects the anode from the electrolyte. This initial loss of Li inventory must be accounted for when designing a battery for proper electrode balancing. Furthermore, morphology of the initial SEI layer significantly impacts performance and longevity of the battery.

The growth of the SEI layer in the PxD electrochemical models is modelled with the Tafel ansatz (e.g., reference [42]) with assumption that SEI grows evenly on the surface of the particles, and which can be written as

$$j^{SEI} = \frac{1}{a^e} A^{SEI} c_{surf}^{EC} \exp\left(-\frac{\alpha^{SEI} F}{RT} \eta^{SEI}\right),$$

where a^e represents specific surface of the active material, A^{SEI} represents SEI formation reaction frequency factor, c_{surf}^{EC} represents concentration of ethylene-carbonate (EC) organic solvent at the particle's surface, α^{SEI} represents charge transfer coefficient for the SEI electrochemical reaction, and finally η^{SEI} represent the overpotential for the SEI formation reaction. The overpotential can be written as

$$\eta^{SEI} = \Phi_s - \Phi_e - U^{SEI} + F \frac{\omega^{SEI} \delta^{film}}{\kappa^{SEI}} j^{tot},$$

where Φ_s and Φ_e represent solid and liquid phase potential, respectively, and couple PxD performance model solutions for both potentials and degradation model. Furthermore, U^{SEI} represents standard potential of SEI layer, ω^{SEI} represents volume fraction of the SEI in the film, where film contains SEI and

plated Li with thickness of δ^{film} and conductivity of SEI layer κ^{SEI}, finally j^{tot} represents total molar flux consisting of intercalation flux and fluxes related to the side reactions. Under the approximation of the thin film compared to the size of an active particle, the c_{surf}^{EC} on the particle's surface can be calculated with the following linearised diffusion equation:

$$D^{EC}\frac{c_0^{EC}-c_{surf}^{EC}}{\delta^{film}}=j^{SEI},$$

where D^{EC} represents diffusion coefficient of EC in the film and c_0^{EC} represent concentration of EC in the bulk electrolyte.

Exhaustive overview of the mechanisms and modelling approaches to the SEI growth can be found in the following references [43, 44, 45].

4.4.4 Plating of the metallic Li

Plating of the metallic Li on the anode's active material is highly undesirable side reaction which occurs when anode potential drops below 0 V vs. Li/Li^+. In this case the plating of Li on the active material's surface is thermodynamically more favourable compared to the intercalation [46, 47]. Certain conditions have to be fulfilled for this phenomenon to occur during charging, namely high charging currents [48], low temperatures [49] and high SoC (i.e. high lithiation levels in the anode particles) [50]. Virtual sensing of the anode potential will play a vital role in the next-generation battery management systems (BMS) in preventing Li-plating under fast charging regime and therefore increasing the longevity and safety of the batteries.

Yang et al. [42] presented one of the first models of Li-plating coupled also with the growth of the SEI layer. The presented model of Li-plating is based on the Tafel equation which implies irreversible loss of cyclable Li during the Li-plating.

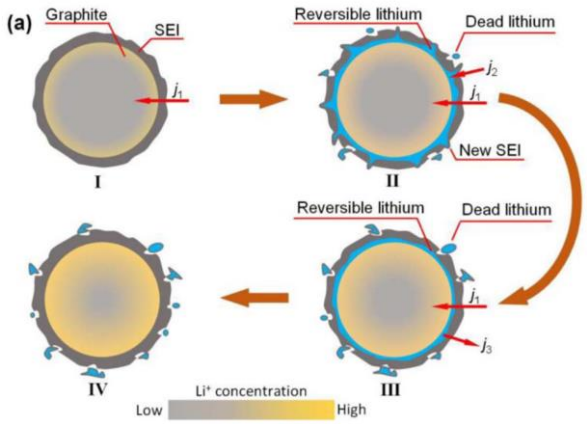

Figure 3. Schematic representation of the Li-plating and Li-stripping. Source [46].

Ren et al. [46] presented an upgraded model which accounts also for reversible Li (so-called Li-stripping phenomenon) alongside the irreversibly lost Li (Figure 3) by utilising the Butler-Volmer equation

$$j^{LPL} = i_0^{LPL}\left(\exp\left(\frac{\alpha_a F}{RT}\eta^{LPL}\right) - \exp\left(\frac{\alpha_c F}{RT}\eta^{LPL}\right)\right)\frac{\beta n_{Li,rev}}{1+\beta n_{Li,rev}},$$

where η^{LPL} represent overpotential for Li-plating and the $\frac{\beta n_{Li,rev}}{1+\beta n_{Li,rev}}$ represents the correction term [46] determining amount of plated Li to be reversibly stripped during discharging of the battery in the electrolyte via the electrochemical reaction.

4.4.5 Mechanical stresses

During (de)lithiation electrode materials experience different volume expansions resulting in mechanical stresses on the level of a single electrochemical model as well as on the battery and module level. The most prominent example of the electrode material with high volume change is Silicon (Si). Due to its high specific capacity (3579 mAh/g) and low open circuit potential against Li/Li+ it is considered as the most rational way to overcome the theoretical capacity limit of the commonly used graphite and to accelerate the development of high energy Li-ion batteries [51]. This is done by combining both materials in different mass fractions resulting in a so-called Si/Graphite blended electrode.

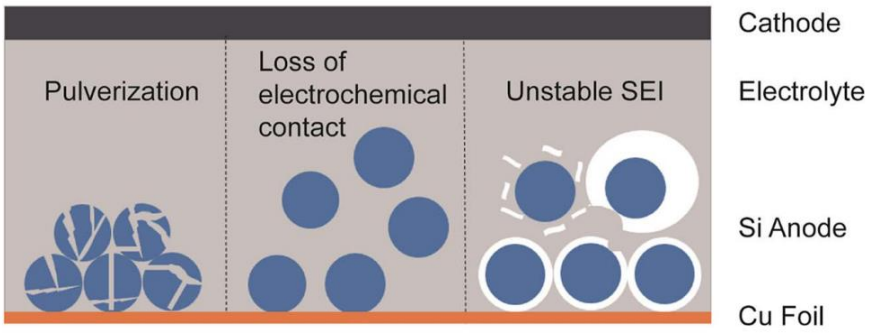

Figure 4. The main degradation processes of Silicon due to its high volume expansion. Source [52].

However, due to the high-volume expansion (see Figure 4) Si particles can crack or pulverize and expose new surface for additional SEI growth and consequent loss of cyclable Li. Furthermore, particles can lose contact with the conduction paths for the electrons [53] and becoming inactive, resulting in capacity loss of the battery. Additionally, repetitive expansions and contraction of silicon particles can damage fragile SEI layer and making it unstable [52]. Yang et al. [54] investigated the effect of weight ratio in the Si/graphite blended electrode and discovered that extent of surface cracking appears to be proportional to the amount of silicon in the electrode.

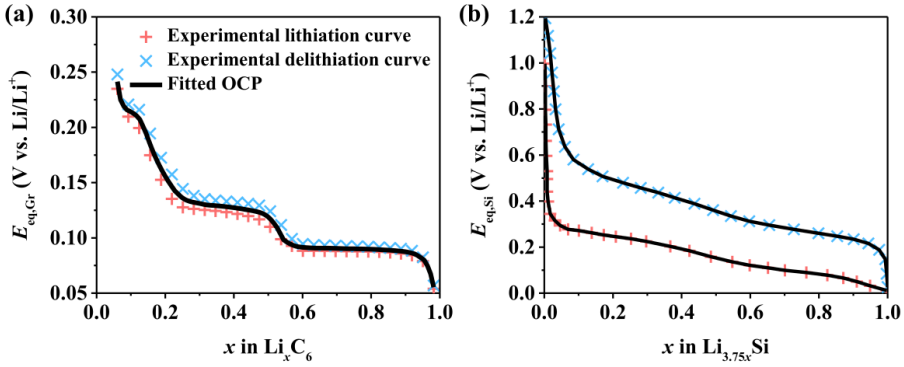

Figure 5. Open circuit potential of (a) graphite and (b) silicon. Source [55].

In a blended electrode, exchange or crosstalk of Li-ions is possible between the electrode materials if the component materials have different working potentials (comparison of OCPs of graphite and Silicon is shown in Figure 5) [56]. During constant-current charging, the silicon tends to be preferentially lithiated. During constant-current discharging graphite is preferentially delithiated until about 50% state-of-charge (SOC) is reached. Silicon then carries the bulk of the charge [54, 56]. It is important therefore that the different open circuit potential of both materials is accounted for to adequately model transport and coupled degradation phenomena due to stress/strain contributions in a blended Si/Graphite electrode.

Modelling of a three-dimensional (3D) physics-based system for Silicon/graphite blended electrodes was performed by Liu et al. [57]. Their detailed model couples electrochemistry and mechanics using as input electrode mesostructures obtained from manufacturing-related Coarse-Grained Molecular Dynamics models [57]. General coupled 1D transport and stress/strain contribution in electrode material k with spherical geometry was proposed by Bonkile et al. [53] and can be modelled with the following equation

$$\frac{dc_k}{dt} = D_k^{eff}\left[\frac{d^2c_k}{dr_k^2} + \frac{2}{r_k}\frac{dc_k}{dr_k} + \Theta_{M,k}\left(\frac{dc_k}{dr_k}\right)^2 + \Theta_{M,k}\bar{c_k}\left(\frac{d^2c_k}{dr_k^2} + \frac{2}{r_k}\frac{dc_k}{dr_k}\right)\right],$$

where the contribution $\Theta_{M,k}$ from stress/strain evaluates as

$$\Theta_{M,k} = \frac{\Omega}{RT}\frac{2\Omega E}{9(1-\nu)}$$

with Ω representing partial molar volume, E representing Young's modulus and ν representing Poisson's ratio.

4.4.6 Gas evolution

Formation of the gaseous species inside the battery is another phenomenon in series of unwanted side reactions. Different gaseous species form in specific electrode due to decomposition of liquid electrolytes used in Li-ion batteries. Reaction depends on the local electrode potential and on whether the electrode is being lithiate or delithiated. For example, CO, C_2H_4, CO_2, and H_2 are formed at negative electrode due to electrolyte reduction, whereas electrolyte oxidation produces CO_2 at the positive electrode [58, 59].

Rashid et al. [60] presented a coupled SEI growth and gas evolution model based on the cathodic Tafel equation:

$$j^{gas} = -\frac{1}{a^e} i_0^{gas} \exp\left(\frac{\alpha_c F}{RT}\eta^{gas}\right),$$

where overpotential for formation of the gaseous species on the anode side is defined as

$$\eta^{gas} = \Phi_s - \Phi_e - U^{gas} + F\frac{\omega^{SEI}\delta^{film}}{\kappa^{SEI}} j^{tot},$$

where similarly as before, Φ_s and Φ_e represent solid and liquid phase potential, respectively and U^{gas} represents standard potential of formation of the gaseous species. Under the assumption that gaseous species fill the electrolyte pores, the change in volume fraction ϵ^{gas} of gaseous species can be calculated with the following equation:

$$\frac{\partial \epsilon^{gas}}{\partial t} = -\frac{j^{gas} V^{gas}}{nF},$$

where V^{gas} represents volume occupied by the gaseous species.

5. MODULE LEVEL MODELLING

This section advances the discourse from individual cells to the complexities of Module Level Modelling. This pivotal section addresses the challenges and methodologies associated with modelling battery modules, where multiple cells interact within a larger, more complex system. Accurate module level modelling is a cornerstone for ensuring the scalability of battery technologies from the laboratory to real-world applications.

It explores an array of modelling techniques tailored to capture the multifaceted dynamics of battery modules. These models must account for the interactions between cells, thermal management requirements, electrical connections, and mechanical constraints, all of which contribute to the overall performance, safety, and durability of the battery module. The section emphasizes the importance of transitioning from cell-specific insights to the broader implications at the module level, ensuring that models can scale up effectively without losing the fidelity of predictions.

5.1 Types of modeling

5.1.1 Thermal analysis

Thermal models of a battery module can be of different types. On the one hand, empirical models are based on experimental data and regression analysis. These models are not based on physical equations, and therefore do not need to be fed by the physical properties of the cells [61]. This can make it difficult to predict thermal behavior when extrapolating operating conditions or cells' physical properties. On the other hand, lumped parameter models simplify heat transfer by means of resistances, capacitances, and thermal loads networks. In this way, the temperature distribution is determined by considering averaged values over the defined elements [62]. Although it may be relatively simple to apply, the thermal results obtained lack spatial resolution. As an alternative, the finite element analysis (FEA) and computational fluid dynamics (CFD) allow the 3D temperature distribution to be evaluated in a more detailed way in more complex geometries [63].

In FEA models only diffusion heat transfer is considered, while CFD models consider the fluid dynamic equations to analyze conjugate heat transfer. Therefore, high-fidelity CFD models are of particular interest when the interaction between a surface and a fluid, such as the cooling system of a battery pack, needs to be analyzed. Usually, the computational cost of CFD models is high. It is worth mentioning that CFD models allow the coupling of physics-based models (PBM) that analyze in detail the electrochemical interactions of the cell, such as the P2D model. However, there is a risk of excessively increasing the cost of the already expensive CFD models. Alternatives have been proposed to reduce this computational cost by use [64].

5.1.2 Mechanical structural analysis

To assess the structural reliability of battery modules, the analysis is focused on the module resistance to shock and vibrational fatigue conditions and finite element methods (FEM) are used for the calculations. To predict the vibrational fatigue resistance, however, further analysis is needed and welded joint geometries, materials and resistance against cyclic loading must be considered.

In [65], a FEM modal analysis of a battery module having prismatic cells is developed. The deformations of the module geometry at natural frequencies are evaluated but a reliability analysis is not performed since the resistance of weak details such as welded joints are not evaluated. The performance of a multi-material battery pack structure is evaluated through random vibration fatigue FEM analysis [66]. The cumulative fatigue damage and lives of each component are predicted but structural weak details such as welded joints are not considered in the analysis. Although different methods for the cyclic loading fatigue analysis of welded joints are exposed in [67], the accuracy of these approaches for vibrational fatigue analysis has not been evaluated yet. Therefore, a method to evaluate the effect of vibrational fatigue in welded joints as the weak points of the battery modules is lacking in the literature.

5.2 Description of electro-thermal model

Maintaining lithium-ion batteries in their optimum temperature range is essential to maximize performance and ensure safety. The most important effects affecting the working temperature of lithium-ion batteries are internal heat generation and environmental conditions [68]. The total internal heat generation in cells is due to the contribution of irreversible and reversible generation. This total generation depends mainly on the applied current, the operating temperature and the state of charge (SOC). Thus, fast charging will generate more heat in the batteries. On the other hand, extreme environmental conditions (hot and/or cold) can affect the working temperature of the cell, leading to accelerated degradation and/or safety problems.

For temperature control, batteries are usually equipped with a battery thermal management system (BTMS). Taking the electric vehicle sector as a reference, at battery module level, the thermal management system (BTMS) usually involves a flow of a fluid (gas or liquid) whose objective is to absorb or provide the desired heat to ensure that the cell is in its optimal temperature range [69]. Thus, the main challenges facing thermal models of lithium-ion batteries at the module level are, on the one hand, the prediction of heat generation under different operating conditions; and on the other hand, the resolution of heat transfer between the active elements (cells) and the fluid.

As previously mentioned, CFD models allow to solve in a coupled way the electrochemical behavior and fluid dynamic equations with a high degree of 3D

spatial resolution. Considering the commercial CFD software Ansys-Fluent, the electrochemical behavior is considered by multi-scale, multi-domain (MSMD) simulations [70]. Among the different MSMD methods, the P2D physics-based model (previously described in section 4.2) provides as a result, among other relevant variables, the internal heat generation [6].

Considering the heat generation obtained from the P2D model, there are several methods to determine the temperature field macroscopically [71] [72]. However, these methods present limitations when the internal gradients in the cell are high, since the heat diffusion is considered to occur homogeneously in the different layers [73]. An alternative proposed in this project are local 3D simulations considering the heterogeneous thermo-physical properties between the different layers of the cell. In this way, considering a thermal model coupled to the P2D model, the generation and the inhomogeneous heat transfer will be considered locally. The local heat diffusion behavior will be extrapolated to the whole cell considering heterogeneous and anisotropic properties in different zones of the cell.

Once the procedure for optimally resolving internal heat generation and diffusion has been defined, the CFD thermal model at the module level must resolve the heat transfer between the heat sources and the fluid. Depending on the method used for thermal management, the level of coupling between heat generation and heat transfer will vary. As an example, the development of the flow of a fluid through a cold plate that is responsible for cooling a battery module can be analyzed with little consideration of coupling between the fluid and the electrochemical behavior of the cell [74]. In this sense, to reduce the high computational cost of CFD models that solve the heat transfer to the fluid (especially in relatively large geometries and/or transient calculations), it is possible to use reduced order methods. Among these MOR techniques for fluid-dynamics simulations, the Lower Order Models Method or order reduction techniques based on modal analysis; and the method based on parametric simulations [75] can be mentioned.

Finally, in this project it is proposed that the final coupled thermal model of the battery module be solved sequentially. The faster dynamics related to the electrochemical behavior of the cells will be solved by reduced order P2D models. The heat generation will be the input of the thermal model of the battery module, with slower dynamics, which will solve the heat transfer to the fluid by reduced order CFD model.

5.3 Description of the mechanical model

Battery structures are subjected to three types of loading conditions [76].On the one hand, to the swelling effect during charge and discharge cycles, where axial stresses are created in the battery structure and connections due to the volumetric changes of the cells. The swelling effect at the beginning (BoL) or at the end (EoL) of the service life may be different. On the other hand, batteries are also exposed to vibrations due to, for example, road irregularities or engine movements during

their life cycle. Vibrational loads can lead to fatigue failure of the battery connections (e.g. welding of terminals) and, therefore, battery life [77]. Finally, battery shocks due to sudden acceleration or deceleration situations that affect the strength of the battery also occur.

While swelling effect varies depending on the battery life, either vibrational loads or shock situations may occur at any moment during the battery life. The swelling effect produces an internal pressure in the battery that affects the behaviour of the battery structure against vibrational fatigue or shock loading conditions. Thus, BoL and EoL battery conditions to be analysed should be defined before shock or vibrational fatigue modelling.

Finite Element Modelling (FEM) method is used for the structural analysis of battery modules and statistical approaches are applied for the lifetime prediction of batteries due to vibrational fatigue loading conditions.

5.3.1 Swelling

Before vibrational and shock analysis are made, a structural preconditioning of modules due to swelling effect of cells must be performed. To do so, a static structural analysis must be carried out modelling the constituent parts of battery modules in terms of geometry and materials [78]. Vibrational and shock analysis will be based on the swelling modelling results.

5.3.2 Vibrational fatigue analysis

For the vibrational fatigue analysis, a modal analysis is necessary after the static structural analysis. Then, the power spectral density (PSD) or the acceleration spectral density (ASD) profile of the load is defined [79] and the stress frequency response function (FRF) of the unitary load [80] is calculated through the harmonic analysis. Afterwards, stress cycles in the frequency domain are calculated using the Probability Density Factor (PDF) methodology [81] [82]. Finally, using S-N or E-N curves the damage (D) caused by the loads in welded connections is evaluated. Connection failure occurs when the damage takes the value 1 and the fatigue life (1/D) of can be calculated. The flowchart for the calculation of fatigue analysis due to random vibrations is shown in Figure 6.

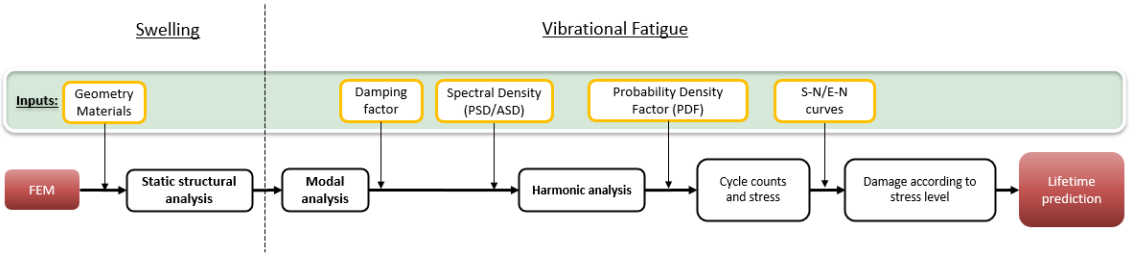

Figure 6. Proposed method for vibrational fatigue analysis.

1. Modal analysis:

Modal analysis allows the identification of specimen resonances and deformation modes. Vibrational fatigue analysis is based on damage due to natural frequency stress spikes in the FRF, so it is necessary to have at least one resonance within the excitation band to cause vibration damage. The participation factor can also be obtained through this analysis, which determines the importance of each deformation mode in the dynamic behaviour of structures.

2. Harmonic analysis:

The stress FRF response under unitary load must be analysed to evaluate the stresses that the structure can withstand as a result of vibrational accelerations. Figure 7 shows the Von Misses stresses that a specific node of the structure would experience at different frequencies due to the acceleration.

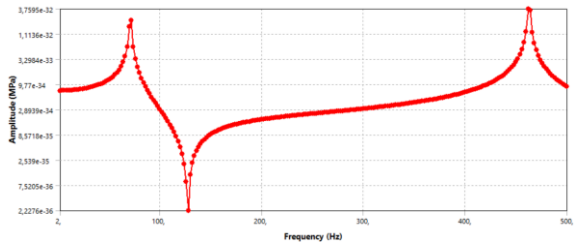

Figure 7. FRF response in a specific node of the structure.

Regarding the FRF of the stress response in Figure 7, stress peaks can be seen at resonances. Although the maxima of these stresses are always found at resonances, the amplitude depends on the damping ratio of the structure [8]. On this way, increasing the damping ratio will reduce peaks and vice versa.

3. Fatigue analysis:

Once the dynamic behaviour of the battery module is analysed, a random vibration input is provided to the model by applying a probability function PDF to obtain an approximation of stress levels. While several methodologies exist to model the PDF (e.g. Dirlik [81], Steinberg Narrow Band or Lalanne [82]), the Dirlik PDF is suggested for vibrational loads. Connecting the vibrational stress results with welded joint's S-N curve, the damage accumulated in the terminal connection due to vibrations can be evaluated. The damage histogram in Figure 8 represents the fatigue damage that each stress interval will produce in the component every second.

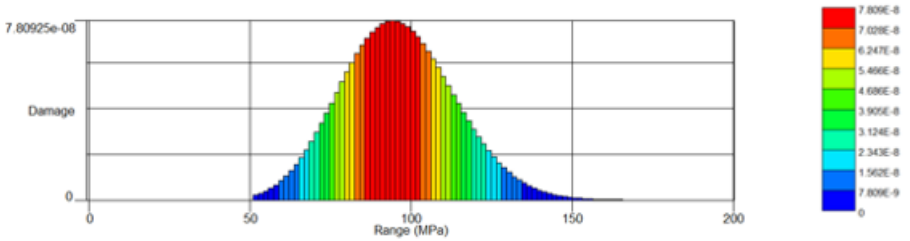

Figure 8. Damage histogram

For the stress analysis in welded joints [83], Hot-Spot [84] or Notch-stress [85] methodologies are applicable. The welded joints are modelled as shown in Figure 9, where the circular path of the welding is simplified as a ring-shape geometry in the overlapped section.

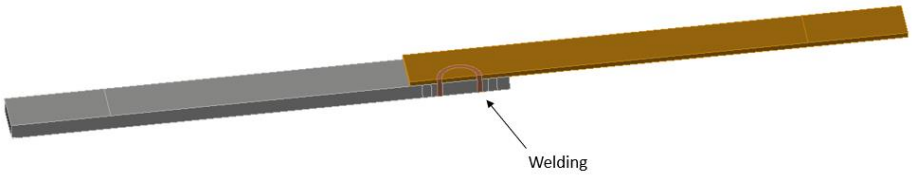

Figure 9. Welded joint modelling

5.3.3 Shock analysis

The battery module to be tested is subjected to shock forces, often analysed as accelerations [76]. While the calculation bases are similar, in the shock analysis fracture occurs due to ultimate stress rather than as a result of fatigue. Thus, the VM stress result obtained through the structural analysis is then compared with the ultimate stress of the welded joint.

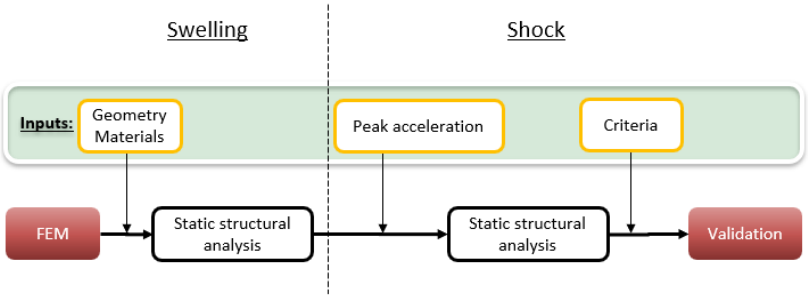

Figure 10. Proposed method for shock analysis

6. FASTEST cell and module level description and models validation

After reviewing the multiscale high-fidelity modelling paradigm that is available in the literature, the specific approach to be followed in the FASTEST project is highlighted for physical testing virtualization. First, the cells and module under study are described. Second, cell level approach is discussed. Finally, the module level approach is assessed.

In the FASTEST project, two types of battery cells with distinctive characteristics will be employed: third-generation cells (3b Generation) and solid-state cells (SSB). These cells have been selected to assess and optimize battery technologies at various stages of the project, reflecting advancements in battery technology and their applicability in real-world contexts.

Third-Generation Cells (3b Generation):

- Cell Type: Pouch
- Cathode: LFP (Lithium Iron Phosphate)
- Anode: SiC (Silicon Carbide)
- Electrolyte: Liquid
- Cell Capacity: 30 Ah
- Nominal Voltage: 3.2 V
- Maximum Voltage: 3.65 V
- Minimum Voltage: 2.2 V
- C-Rate (Discharge): 0.5C
- Operating Temperature: 0 to 50 °C
- Weight: 0.3 to 0.35 Kg

The third-generation cells offer a balance between safety, capacity, and efficiency. The choice of LFP cathode and SiC anode prioritizes thermal stability and longevity, crucial aspects for high-reliability applications.

Solid-State Cells (SSB):

- Cell Type: Pouch
- Cathode: LFP
- Anode: SiC
- Electrolyte: Solid state (polymer-based)
- Cell Capacity: 30 Ah
- Nominal Voltage: 3.2 V
- Maximum Voltage: 3.65 V
- Minimum Voltage: 2.2 V
- Discharge Rate: 0.5C
- Charge Rate: 0.5C
- Operating Temperature: 10 to 60 °C
- Weight: 0.4 Kg

SSB cells represent an innovation in battery technology, offering increased safety and energy density thanks to their solid-state electrolyte. This feature is particularly attractive for applications requiring high energy density and greater tolerance to higher temperatures.

The use of these two cell technologies in the FASTEST project provides a platform to evaluate and compare the performance, safety, and feasibility of emerging battery technologies in practical applications.

6.1 Model Validation at cell level

Non-invasive tests are based on electrical, electrochemical or thermal tests. Voltage, current and temperature data are commonly acquired. The equipment necessary for these validations generally requires a cycler, a climatic chamber, a thermocouple and sometimes a potentiostat. All the works presented in Table 2 have been taken as a reference to study the tests that are usually used for a P2D model validation. The summary of the analysis is presented in Table 2. These tests could be divided into three categories: capacity tests (galvanostatic or potentiostatic charge discharge cycles at different DoD, current rates and temperatures), dynamic tests (pulse tests at different current rates, SoCs, temperatures, standard HPPC tests, EIS tests, realistic profiles) and temperature validation tests.

Table 2. P2D model non-invasive validation methods.

Non-invasive test	Doyle 1996 [7]	Doyle 2003 [5]	Fang 2010 [86]	Safari 2011 [87]	Prada 2012 [88]	Ecker 2015 [89]	Schmalstieg 2017 [90]	Falconi 2018 [91]
CC_{dch} (C_{rate}, T)	T_{25}	T_{25}	T_{r1}	T_{25}	T_{r2}	T_{r3}	T_{r3}	T_{25}
CC_{cha} (C_{rate}, T)	-	T_{25}	T_{r1}	T_{25}	T_{r2}	T_{r3}	T_{r3}	T_{25}
Pulse (C_{rate}, SoC, T)	-	-	T_{r1}	-	-	T_{r3}	T_{r3}	-
EIS (SoC, T)	-	-	-	-	-	-	T_{r3}	-
R_{drive}	-	-	-	-	-	-	T_{r3}	-
T_{surf}	-	-	T_{25}	-	T_{r2}	-	T_{r3}	-

CC_{dch}: Validation with galvanostatic discharge process at different current rates.

CC_{cha}: Validation with galvanostatic charge process at different current rates.

Pulse: Validation with pulse power charges/discharges at different C-rates and SoCs.

EIS: Validation with Electrochemical impedance spectroscopy tests at different SoCs.

R_{drive}: Realistic driving profile.

T_{surf} : Validation with cell surface temperature; T_{25}: Temperature control at 25 _C;

T_{r1}: Temperature control between 0 and 25 _C; T_{r2}: Temperature control between 0 to 33 _C; T_{r3}: Temperature control between -10 to 40 _C.

In Table 2 all authors validate their results against capacity tests. However, only some of them validate the dynamic responses of the model [86, 90, 91]. Some of the works also present battery surface temperature validation, which corresponds to the addition of a fifth PDE (energy balance equation) into the P2D model and its validation. Schmalstieg et al. [90] provided the most complete work between the analysed research.

A good experimental-numerical match in those results describes the behaviour of cells and model validity at different operating conditions. However, to use those models for internal variable control (overvoltage evolution, ageing evolution etc.) it is necessary to ensure that the model predictions are in good concordance with the experimental evolution.

6.1.1 Capacity retention

Capacity retention measurement during battery cycling is the most basic and non-destructive method commonly used to study averaged battery degradation (example shown on Figure 11). Measuring of the remaining capacity is performed with low C-rates to avoid high overpotentials, e.g. C/10, in-between the cycling, where the cycling C-rates are usually higher in order to accelerate the aging process and reduce the measurement time.

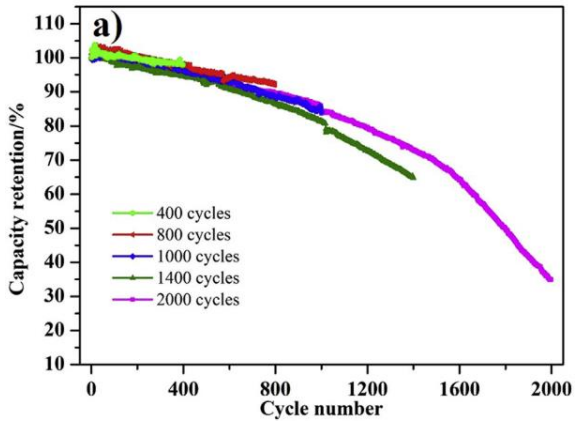

Figure 11. Example of capacity retention measurement on LFP/Graphite cells. Source [39].

Loss of cyclable lithium can be ascribed to several processes and can be written in a generalised manner

$$C_{loss}(t_0) = FV \int_0^{t_0} [a_e \sum_i j_{i,deg}] dt,$$

where C_{loss} represents capacity loss at time t_0, F represents Faraday constant, V represents volume of the electrochemical cell, a_e represents averaged specific surface of the active material in the electrode and $j_{i,deg}$ represents molar fluxes of the side-reactions, e.g. for SEI growth, Li-plating, etc.

6.1.2 EIS measurements

Electrochemical impedance spectroscopy (EIS) is a powerful method for non-invasive monitoring of intra-cell phenomena for characterising electrochemical devices such as Li-ion batteries [92, 93]. The main idea of this method is to apply a small potential (potentiostatic EIS or PEIS) or a small current (galvanostatic EIS or GEIS) excitation to the electrochemical device in the form of a sinusoidal perturbation with frequencies ranging across several orders of magnitude [93] (typically from kHz to mHz) and measure its response, i.e., amplitude and phase shift. The result is an impedance spectrum presented with a Nyquist diagram that characterises the phenomena in the battery that occur on the different time scales.

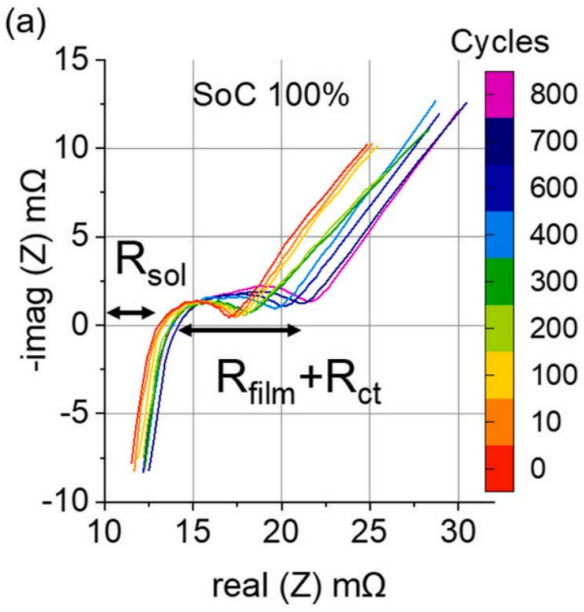

Figure 12. Example of the evolution of the impedance spectra of a Li-ion battery during the electrochemical cycling. Source [94].

Figure 12 demonstrates an example how the impedance spectra of a Li-ion battery evolves with increasing number of cycles. Can be easily seen from Figure 12 that the overall impedance increases. More precisely, the intersection of the EIS spectra with the Re(Z) axis at high frequencies indicates the increase of the internal resistance of the battery. Furthermore, the semi-circle that corresponds to the

charge transfer resistance and resistance of the passivated film expands quite significantly indicating presence of the degradation processes.

The EIS protocol can be mimicked also virtually with the full electrochemical model in time domain by applying sinusoidal current or voltage boundary condition at the current collector/electrode interface. In the literature, there aren't many papers that use such approach. R-Smith et al. [94] modelled EIS spectra with the COMSOL Multiphysics of the full commercial cell at different levels of degradation and extracted several ageing parameters, supported by the advanced microscopy techniques.

It has to be noted that interpretation of the EIS spectra is very challenging since there are many intra-cell phenomena occurring at similar timescales and are superimposed in the resulting EIS spectra, especially in the case of the full cell with two insertion electrodes.

6.1.3 Advanced post-mortem microscopy

Advanced microscopy methods such as FIB-SEM or TEM are classified as a destructive since cells are disassembled in the process. However, they provide valuable insights into the intra-cell state in fresh and degraded state. For example, morphology of the electrode, size distribution of the primary and secondary active particles, cracks in the particles, particle connectivity, etc. Such microscopy results are not directly used for model validation but serve as a model parameterisation and guidance in model development. For example, Scipioni et al. [95] performed FIB-SEM tomography analysis which revealed that the anode graphite particle size is smaller in size in the cycled battery compared to the fresh battery whereas no significant change in cathode LFP particle size could be observed. They concluded that the decrease in the graphite particle size could be an effect of mechanical stress during lithiation/delithiation process [95].

6.2 Model validation at module level

Two different model validations are defined: Thermal analysis part and mechanical structural analysis part.

To validate the results of the thermal model, the results of the electrothermal characterization of the battery module will be used. The thermal tests will consist of fast and deep charges/discharges; and stationary pulse tests at different C-ratios, SOC levels and ambient conditions. The reference results will be:

- The heat absorbed by the fluid (validating the heat generation models and heat transfer to the fluid).
- The temperature distribution in reference cells of the module (validating the heat diffusion results in the internal cell layers).
- The temperatures in the prismatic elements and electrical connections (validating the heat transfer in the auxiliary elements).

To validate mechanical structural analysis part, vibrational fatigue results of welded joint, first an experimental modal analysis and, second, vibrational fatigue tests

must be carried out [76].While modal tests are used for the validation of the resonances and the characterization of the dampi ng ratio, vibrational fatigue tests will characterise the dynamic behaviour and durability of welded joints [96].

A shaker test bench will provide the vibrational input to welded joints, and the dynamic behaviour of welded joints will be characterised by using accelerometers attached to test specimens [97].

7. CONCLUSION

At cell level, different electrochemical models at continuum scale (P2D, SPM, SPMe) are presented. Those models could be simplified or reduced to fasten the computational time without losing accuracy. We highly recommend the use of model order reduction techniques and simplifications to decrease the complexity of electrochemical models, enabling real-time implementation while retaining physical information. By preserving the parameters of full-order models, significant reductions in time and computational load for optimisations in the estimation process can be achieved. This will be developed thereafter in the FASTEST project.

To enhance the electrochemical model, thermal and ageing contributions should be added. The cell format is already defined, so it should be carefully check the accuracy of the Bernardi equation on 0D and the temperature model at cell level when large format of cells is used. This simplified thermal model will be replaced with advanced approaches when 3D-thermal battery modules are proposed. The physics-based models are claimed to be helpful in order to get the physical insights of the battery cells as well as to build enhanced 3D-thermal battery module models with cell physics-based model inputs. For thermal cell and module models it is critical to assess whether external cooling will be applied or natural convection. This is linked to the application of the module and is addressed in other deliverables of the project, in which use case specifications are defined.

The modelling of degradation phenomena in batteries is inherently intertwined with performance and thermal models, which provide inputs such as potentials and temperature to the degradation models. The main degradation phenomena (e.g. growth of the SEI layer, plating of the metallic Li, mechanical stresses, gas evolution, etc.) and corresponding modelling approaches for Li-ion batteries with LFP cathode and Si/Graphite blended anode were presented. The validation of such models is a challenge as advanced post-mortem microscopy is required to gain insights into the intra-cell state of fresh and degraded cells, e.g. morphology of the electrode, size distribution of primary and secondary active particles, cracks in the particles, particle connectivity.

8. Bibliography

[1] F. B. Planella, „A continuum of physics-based lithium-ion battery models reviewed," Prog. Energy 4 042003, June 2022. [Online]. Available: https://iopscience.iop.org/article/10.1088/2516-1083/ac7d31#:~:text=Continuum%20battery%20models%20generally%20fall,observable%20behaviour%20of%20the%20battery.

[2] S. F. S. M. E. G. F. A. F. Ehsan Samadani, „Empirical Modeling of Lithium-ion Batteries Based on Electrochemical Impedance Spectroscopy Tests," Elsevier, 2015. [Online]. Available: https://www.sciencedirect.com/science/article/abs/pii/S0013468615002984#.

[3] M. S. Y. K. L. K. K. E. J. L. Malin Andersson, „Sciencedirect," Elsevier, 2022. [Online]. Available: https://www.sciencedirect.com/science/article/pii/S0378775321013458#.

[4] A. S. A.-K. S. H. H. A. E. Mohamed A. Abu-Seif, „Data-Driven modeling for Li-ion battery using dynamic mode decomposition," Alexandria Engineering Journal, 2022. [Online]. Available: https://www.sciencedirect.com/science/article/pii/S111001682200299X#.

[5] M. Doyle en Y. Fuentes, „Computer simulations of a lithium-ion polymer battery and implications for higher capacity next-generation battery designs," *Journal of The Electrochemical Society,* vol. 150, p. A706, 2003.

[6] M. Doyle, T. F. Fuller en J. Newman, „Modeling of galvanostatic charge and discharge of the lithium/polymer/insertion cell," *Journal of the Electrochemical society,* vol. 140, p. 1526, 1993.

[7] M. Doyle, J. Newman, A. S. Gozdz, C. N. Schmutz en J.-M. Tarascon, „Comparison of modeling predictions with experimental data from plastic lithium ion cells," *Journal of the Electrochemical Society,* vol. 143, p. 1890, 1996.

[8] M. Doyle en J. Newman, „The use of mathematical modeling in the design of lithium/polymer battery systems," *Electrochimica Acta,* vol. 40, p. 2191–2196, 1995.

[9] G. L. Plett, Battery management systems, Volume I: Battery modeling, vol. 1, Artech House, 2015.

[10] R. Darling en J. Newman, „Modeling a porous intercalation electrode with two characteristic particle sizes," *Journal of The Electrochemical Society,* vol. 144, p. 4201, 1997.

[11] F. Röder, S. Sonntag, D. Schröder en U. Krewer, „Simulating the impact of particle size distribution on the performance of graphite electrodes in lithium-ion batteries," *Energy Technology,* vol. 4, p. 1588–1597, 2016.

[12] S. T. Taleghani, B. Marcos, K. Zaghib en G. Lantagne, „A study on the effect of porosity and particles size distribution on Li-ion battery performance," *Journal of The Electrochemical Society,* vol. 164, p. E3179, 2017.

[13] M. Farkhondeh en C. Delacourt, „Mathematical modeling of commercial LiFePO4 electrodes based on variable solid-state diffusivity," *Journal of The Electrochemical Society,* vol. 159, p. A177, 2011.

[14] Z. Mao, M. Farkhondeh, M. Pritzker, M. Fowler en Z. Chen, „Multi-particle model for a commercial blended lithium-ion electrode," *Journal of The Electrochemical Society,* vol. 163, p. A458, 2015.

[15] A. Bartlett, J. Marcicki, S. Onori, G. Rizzoni, X. G. Yang en T. Miller, „Electrochemical model-based state of charge and capacity estimation for a composite electrode lithium-ion battery," *IEEE Transactions on control systems technology,* vol. 24, p. 384–399, 2015.

[16] M. Petit, E. Calas en J. Bernard, „A simplified electrochemical model for modelling Li-ion batteries comprising blend and bidispersed electrodes for high power applications," *Journal of Power Sources,* vol. 479, p. 228766, 2020.

[17] S. Carelli, M. Quarti, M. C. Yagci en W. G. Bessler, „Modeling and experimental validation of a high-power lithium-ion pouch cell with LCO/NCA blend cathode," *Journal of The Electrochemical Society,* vol. 166, p. A2990, 2019.

[18] Y. Li, D. Karunathilake, D. M. Vilathgamuwa, Y. Mishra, T. W. Farrell, C. Zou en others, „Model order reduction techniques for physics-based

lithium-ion battery management: A survey," *IEEE Industrial Electronics Magazine,* vol. 16, p. 36–51, 2021.

[19] S. Santhanagopalan, Q. Guo, P. Ramadass en R. E. White, „Review of models for predicting the cycling performance of lithium ion batteries," *Journal of power sources,* vol. 156, p. 620–628, 2006.

[20] S. G. Marquis, V. Sulzer, R. Timms, C. P. Please en S. J. Chapman, „An asymptotic derivation of a single particle model with electrolyte," *Journal of The Electrochemical Society,* vol. 166, p. A3693, 2019.

[21] S. K. Rahimian, S. Rayman en R. E. White, „Extension of physics-based single particle model for higher charge–discharge rates," *Journal of Power Sources,* vol. 224, p. 180–194, 2013.

[22] J. Li, K. Adewuyi, N. Lotfi, R. G. Landers en J. Park, „A single particle model with chemical/mechanical degradation physics for lithium ion battery State of Health (SOH) estimation," *Applied energy,* vol. 212, p. 1178–1190, 2018.

[23] F. B. Planella en W. D. Widanage, „A Single Particle model with electrolyte and side reactions for degradation of lithium-ion batteries," *Applied Mathematical Modelling,* vol. 121, p. 586–610, 2023.

[24] F. B. Planella, M. Sheikh en W. D. Widanage, „Systematic derivation and validation of a reduced thermal-electrochemical model for lithium-ion batteries using asymptotic methods," *Electrochimica Acta,* vol. 388, p. 138524, 2021.

[25] Y. Ye, Y. Shi, N. Cai, J. Lee en X. He, „Electro-thermal modeling and experimental validation for lithium ion battery," *Journal of Power Sources,* vol. 199, p. 227–238, 2012.

[26] C. Fink en B. Kaltenegger, „Electrothermal and electrochemical modeling of lithium-ion batteries: 3D simulation with experimental validation," *ECS Transactions,* vol. 61, p. 105, 2014.

[27] G. Liebig, G. Gupta, U. Kirstein, F. Schuldt en C. Agert, „Parameterization and validation of an electrochemical thermal model of a lithium-ion battery," *Batteries,* vol. 5, p. 62, 2019.

[28] C. R. Pals en J. Newman, „Thermal modeling of the lithium/polymer battery: I. Discharge behavior of a single cell," *Journal of the Electrochemical Society,* vol. 142, p. 3274, 1995.

[29] C. R. Pals en J. Newman, „Thermal modeling of the lithium/polymer battery: II. Temperature profiles in a cell stack," *Journal of the Electrochemical Society,* vol. 142, p. 3282, 1995.

[30] D. Bernardi, E. Pawlikowski en J. Newman, „A general energy balance for battery systems," *Journal of the electrochemical society,* vol. 132, p. 5, 1985.

[31] A. M. Bizeray, J. Kim, S. R. Duncan en D. A. Howey, „Identifiability and parameter estimation of the single particle lithium-ion battery model," *IEEE Transactions on Control Systems Technology,* vol. 27, p. 1862–1877, 2018.

[32] G. G. Botte, B. A. Johnson en R. E. White, „Influence of some design variables on the thermal behavior of a lithium-ion cell," *Journal of the Electrochemical Society,* vol. 146, p. 914, 1999.

[33] W. B. Gu en C. Y. Wang, „Thermal-electrochemical modeling of battery systems," *Journal of The Electrochemical Society,* vol. 147, p. 2910, 2000.

[34] G. Zhang, L. Cao, S. Ge, C.-Y. Wang, C. E. Shaffer en C. D. Rahn, „In situ measurement of radial temperature distributions in cylindrical Li-ion cells," *Journal of the electrochemical society,* vol. 161, p. A1499, 2014.

[35] X. Hu, L. Xu, X. Lin en M. Pecht, „Battery lifetime prognostics," *Joule,* vol. 4, p. 310–346, 2020.

[36] T. Katrašnik, I. Mele en K. Zelič, „Multi-scale modelling of Lithium-ion batteries: From transport phenomena to the outbreak of thermal runaway," *Energy Conversion and Management,* vol. 236, p. 114036, 2021.

[37] I. Mele, I. Pačnik, K. Zelič, J. Moškon en T. Katrašnik, „Advanced porous electrode modelling framework based on more consistent virtual representation of the electrode topology," *Journal of The Electrochemical Society,* vol. 167, p. 060531, 2020.

[38] T. Katrašnik, J. Moškon, K. Zelič, I. Mele, F. Ruiz-Zepeda en M. Gaberšček, „Entering Voltage Hysteresis in Phase-Separating Materials: Revealing the Electrochemical Signature of the Intraparticle Phase-Separated State," *Advanced Materials,* p. 2210937, 2023.

[39] M. Rao, L. Zhang, L. Li, L. Rong, C. Ye, G. Zhou, H. Xu en Y. Qiu, „Investigation of lithium content changes to understand the capacity fading mechanism in LiFePO4/graphite battery," *Journal of Electroanalytical Chemistry,* vol. 853, p. 113544, 2019.

[40] S. Sun, T. Guan, X. Cheng, P. Zuo, Y. Gao, C. Du en G. Yin, „Accelerated aging and degradation mechanism of LiFePO 4/graphite batteries cycled at high discharge rates," *RSC advances,* vol. 8, p. 25695–25703, 2018.

[41] M. Esmaeilpour, S. Jana, H. Li, M. Soleymanibrojeni en W. Wenzel, „A Solution-Mediated Pathway for the Growth of the Solid Electrolyte Interphase in Lithium-Ion Batteries," *Advanced Energy Materials,* vol. 13, p. 2203966, 2023.

[42] X.-G. Yang, Y. Leng, G. Zhang, S. Ge en C.-Y. Wang, „Modeling of lithium plating induced aging of lithium-ion batteries: Transition from linear to nonlinear aging," *Journal of Power Sources,* vol. 360, p. 28–40, 2017.

[43] A. Wang, S. Kadam, H. Li, S. Shi en Y. Qi, „Review on modeling of the anode solid electrolyte interphase (SEI) for lithium-ion batteries," *npj Computational Materials,* vol. 4, p. 15, 2018.

[44] E. Peled en S. Menkin, „SEI: past, present and future," *Journal of The Electrochemical Society,* vol. 164, p. A1703, 2017.

[45] B. Horstmann, F. Single en A. Latz, „Review on multi-scale models of solid-electrolyte interphase formation," *Current Opinion in Electrochemistry,* vol. 13, p. 61–69, 2019.

[46] D. Ren, K. Smith, D. Guo, X. Han, X. Feng, L. Lu, M. Ouyang en J. Li, „Investigation of lithium plating-stripping process in Li-ion batteries at low temperature using an electrochemical model," *Journal of The Electrochemical Society,* vol. 165, p. A2167, 2018.

[47] C. von Lüders, J. Keil, M. Webersberger en A. Jossen, „Modeling of lithium plating and lithium stripping in lithium-ion batteries," *Journal of Power Sources,* vol. 414, p. 41–47, 2019.

[48] J. Fan en S. Tan, „Studies on charging lithium-ion cells at low temperatures," *Journal of The Electrochemical Society,* vol. 153, p. A1081, 2006.

[49] J. C. Burns, D. A. Stevens en J. R. Dahn, „In-situ detection of lithium plating using high precision coulometry," *Journal of the Electrochemical Society,* vol. 162, p. A959, 2015.

[50] T. Waldmann, M. Kasper en M. Wohlfahrt-Mehrens, „Optimization of charging strategy by prevention of lithium deposition on anodes in high-energy lithium-ion batteries–electrochemical experiments," *Electrochimica Acta,* vol. 178, p. 525–532, 2015.

[51] M. Choi, J. Sung, G. Yeo, S. Chae en M. Ko, „A strategy of boosting the effect of carbon nanotubes in graphite-blended Si electrodes for high-energy lithium-ion batteries," *Journal of Energy Storage,* vol. 72, p. 108301, 2023.

[52] B. Zhu, X. Wang, P. Yao, J. Li en J. Zhu, „Towards high energy density lithium battery anodes: silicon and lithium," *Chemical science,* vol. 10, p. 7132–7148, 2019.

[53] M. P. Bonkile, Y. Jiang, N. Kirkaldy, V. Sulzer, R. Timms, H. Wang, G. Offer en B. Wu, „Coupled electrochemical-thermal-mechanical stress modelling in composite silicon/graphite lithium-ion battery electrodes," *Journal of Energy Storage,* vol. 73, p. 108609, 2023.

[54] Z. Yang, M. Kim, L. Yu, S. E. Trask en I. Bloom, „Chemical Interplay of Silicon and Graphite in a Composite Electrode in SEI Formation," *ACS applied materials & interfaces,* vol. 13, p. 56073–56084, 2021.

[55] Y. Jiang, Z. Niu, G. Offer, J. Xuan en H. Wang, „Insights into the role of silicon and graphite in the electrochemical performance of silicon/graphite blended electrodes with a multi-material porous electrode model," *Journal of The Electrochemical Society,* vol. 169, p. 020568, 2022.

[56] J. Moon, H. C. Lee, H. Jung, S. Wakita, S. Cho, J. Yoon, J. Lee, A. Ueda, B. Choi, S. Lee en others, „Interplay between electrochemical reactions and

mechanical responses in silicon–graphite anodes and its impact on degradation," *Nature Communications,* vol. 12, p. 2714, 2021.

[57] C. Liu, O. Arcelus, T. Lombardo, H. Oularbi en A. A. Franco, „Towards a 3D-resolved model of Si/Graphite composite electrodes from manufacturing simulations," *Journal of Power Sources,* vol. 512, p. 230486, 2021.

[58] J. H. Seo, J. Park, G. Plett en A. M. Sastry, „Gas-evolution induced volume fraction changes and their effect on the performance degradation of Li-ion batteries," *Electrochemical and Solid-State Letters,* vol. 13, p. A135, 2010.

[59] J.-S. Shin, C.-H. Han, U.-H. Jung, S.-I. Lee, H.-J. Kim en K. Kim, „Effect of Li2CO3 additive on gas generation in lithium-ion batteries," *Journal of power sources,* vol. 109, p. 47–52, 2002.

[60] M. Rashid en A. Gupta, „Mathematical model for combined effect of SEI formation and gas evolution in Li-ion batteries," *ECS Electrochemistry Letters,* vol. 3, p. A95, 2014.

[61] S. Hoelle, F. Dengler , S. Zimmermann en O. Hinrichsen, „3D Thermal Simulation of Lithium-Ion Battery Thermal Runaway in Autoclave Calorimetry: Development and Comparison of Modeling Approaches," *Journal of The Electrochemical Society,* vol. 170, nr. 1, p. 010509, 2023.

[62] X. Cui, „Online temperature distribution estimation of lithium-ion battery considering non-uniform heat generation characteristics under boundary cooling," *Applied Thermal Engineering,* vol. 225, p. 120206, 2023.

[63] H. A. Hasan, H. Togun, H. I. Mohammed, A. M. Abed en R. Z. Homod, „CFD simulation of effect spacing between lithium-ion batteries by using flow air inside the cooling pack," *Journal of Energy Storage,* vol. 72, nr. D, p. 108631, 2023.

[64] G. Zhu, C. Kong, J. V. Wang, J. Kang, G. Yang en Q. Wang, „A fractional-order model of lithium-ion battery considering polarization in electrolyte and thermal effect," *Electrochimica Acta,* vol. 438, p. 141461, 2023.

[65] F. L. C. X. Y. L. Y. L. W. Z. W. W. B. Xia, „Experimental and simulation modal analysis of prismatic battery module," *Energies,* p. 13, 2020.

[66] „Hye-gyu Kim et al 2021 Funct. Compos. Struct. 3 025006".

[67] „'DesignLife Theory Guide', 2013.," [Online]. Available: Available: www.hbm.com/ncode.

[68] J. Lin, X. Liu, S. Li, C. Zhang en S. Yang, „A review on recent progress, challenges and perspective of battery thermal management system," *International Journal of Heat and Mass Transfer,* vol. 167, p. 120834, 2021.

[69] V. Mali, R. Saxena, K. Kumar, A. Kalam en B. Tripathi, „Review on battery thermal management systems for energy-efficient electric vehicles," *Renewable and Sustainable Energy Reviews,* vol. 151, p. 111611, 2021.

[70] ANSYS, Inc., Ansys Fluent Theory Guide, Canonsburg, PA (USA): ANSYS, Inc., 2022.

[71] D. Kang, P.-Y. Lee, K. Yoo en J. Kim, „Internal thermal network model-based inner temperature distribution of high-power lithium-ion battery packs with different shapes for thermal management," *Journal of Energy Storage,* vol. 27, p. 101017, 2020.

[72] Y. Z. Zeng, D. Chalise, S. D. Lubner, S. Kaur en R. S. Prasher, „A review of thermal physics and management inside lithium-ion batteries for high energy density and fast charging," *Energy Storage Materials,* vol. 41, pp. 264-288, 2021.

[73] M. Chen, F. Bai, W. Song, J. Lv, S. Lin, Z. Feng, Y. Li en Y. Ding, „A multilayer electro-thermal model of pouch battery during normal discharge and internal short circuit process," *Applied Thermal Engineering,* vol. 120, pp. 506-516, 2017.

[74] S. A. Jayarajan en U. Azimov, „CFD Modeling and Thermal Analysis of a Cold Plate Design with a Zig-Zag Serpentine Flow Pattern for Li-Ion Batteries," *Energies,* vol. 16, nr. 14, p. 5243, 2023.

[75] X. Gao, Y. Ma en H. Chen, „Active Thermal Control of a Battery Pack Under Elevated Temperatures," *IFAC-PapersOnLine,* vol. 51, nr. 31, pp. 262-267, 2018.

[76] „V. Ruiz, A. Pfrang, A. Kriston, N. Omar, P. Van den Bossche, and L. Boon-Brett, 'A review of international abuse testing standards and regulations for lithium ion batteries in electric and hybrid electric vehicles', Renewable and Sustainable Energy Review".

[77] „N. Kumar, I. Masters, and A. Das, 'In-depth evaluation of laser-welded similar and dissimilar material tab-to-busbar electrical interconnects for electric vehicle battery pack', J Manuf Process, vol. 70, pp. 78–96, Oct. 2021, doi: 10.1016/j.jmapro.2021.08".

[78] „M. Alexy, D. van de Wall, G. Shannon, and M. L. Boyle, 'Batteries need strong connections – are resistance, laser and micro TIG welding the best suited joining technologies?', Biuletyn Instytutu Spawalnictwa, vol. 2019, no. 1, pp. 53–63, 2019, doi: 10.177".

[79] „Y. Taiwen, 'Synthesis of random vibration environment spectra for the fatigue analysis', Int J Fatigue, 2022, doi: 10.1016/j.ijfatigue.2022.106752.".

[80] „J. P. Quigley, Y. L. Lee, and L. Wang, 'Review and Assessment of Frequency-Based Fatigue Damage Models', SAE International Journal of Materials and Manufacturing, vol. 9, no. 3, pp. 565–577, Apr. 2016, doi: 10.4271/2016-01-0369".

[81] „'DesignLife Theory Guide', 2013. [Online]. Available: www.hbm.com/ncode".

[82] „Christian. Lalanne, Mechanical vibration and shock analysis Fatigue Damage, vol. 4. 2014".

[83] „R. Kristiansson and F. Norberg, 'Fatigue Life Prediction in Aluminium Welds for Thin-sheet Structures', Chalmers University of Technology, 2022".

[84] „M. Aygül, 'Fatigue Analysis of Welded Structures Using the Finite Element Method'".

[85] „A. F. Hobbacher, 'IIW Collection Recommendations for Fatigue Design of Welded Joints and Components'. [Online]. Available: http://www.springer.com/series/13906".

[86] W. Fang, O. J. Kwon en C.-Y. Wang, „Electrochemical–thermal modeling of automotive Li-ion batteries and experimental validation using a three-electrode cell," *International journal of energy research,* vol. 34, p. 107–115, 2010.

[87] M. Safari en C. Delacourt, „Mathematical modeling of lithium iron phosphate electrode: galvanostatic charge/discharge and path dependence," *Journal of The Electrochemical Society,* vol. 158, p. A63, 2010.

[88] E. Prada, D. Di Domenico, Y. Creff, J. Bernard, V. Sauvant-Moynot en F. Huet, „Simplified electrochemical and thermal model of LiFePO4-graphite Li-ion batteries for fast charge applications," *Journal of The Electrochemical Society,* vol. 159, p. A1508, 2012.

[89] M. Ecker, Lithium Plating in Lithium-Ion Batteries, vol. 80, Aachen: Shaker Verlag, 2016.

[90] J. Schmalstieg, „Physikalisch-elektrochemische simulation von lithium-ionen-batterien: implementierung, parametrierung und anwendung," 2017.

[91] A. Falconi, „Electrochemical Li-Ion battery modeling for electric vehicles," 2017.

[92] F. Ciucci, „Modeling electrochemical impedance spectroscopy," *Current Opinion in Electrochemistry,* vol. 13, p. 132–139, 2019.

[93] N. Meddings, M. Heinrich, F. Overney, J.-S. Lee, V. Ruiz, E. Napolitano, S. Seitz, G. Hinds, R. Raccichini, M. Gaberšček en others, „Application of electrochemical impedance spectroscopy to commercial Li-ion cells: A review," *Journal of Power Sources,* vol. 480, p. 228742, 2020.

[94] N. A.-Z. R-Smith, M. Leitner, I. Alic, D. Toth, M. Kasper, M. Romio, Y. Surace, M. Jahn, F. Kienberger, A. Ebner en others, „Assessment of lithium ion battery ageing by combined impedance spectroscopy, functional microscopy and finite element modelling," *Journal of Power Sources,* vol. 512, p. 230459, 2021.

[95] R. Scipioni, P. S. Jørgensen, D. I. Stroe, R. Younesi, S. B. Simonsen, P. Norby, J. Hjelm en S. H. Jensen, „Complementary analyses of aging in a

commercial LiFePO4/graphite 26650 cell," *Electrochimica Acta,* vol. 284, p. 454–468, 2018.

[96] „F. Mocera, A. Somà, D. Clerici, Study of aging mechanisms in lithium-ion batteries for working vehicle applications. XV International Conference on Ecological Vehicles and Renewable Energies (EVER), 2020.".

[97] *D. Marques, D. Vandepitte, V. Tita. Structural health monitoring for damage detection and fatigue life estimation: A frequency-domain approach. VAL4 Fourth International Conference on Material and Component Performance Under Variable Amplitude Loading.*